Available online at www.sciencedirect.com

SciVerse ScienceDirect

Ceramics International 38 (2012) 6289–6294

CERAMICS INTERNATIONAL

www.elsevier.com/locate/ceramint

Potential red-emitting $NaGd(MO_4)_2$:R (M = W, Mo, R = Eu^{3+}, Sm^{3+}, Bi^{3+}) phosphors for white light emitting diodes applications

Fuwang Mo[a], Liya Zhou[a,*], Qi Pang[b], Fuzhong Gong[a], Zhijuan Liang[a]

[a]School of Chemistry and Chemical Engineering, Guangxi University, Nanning 530004, China
[b]Department of Chemistry and Biology, Yulin Normal University, Yulin 537000, People's Republic of China

Received 31 March 2012; received in revised form 11 April 2012; accepted 30 April 2012
Available online 9 May 2012

Abstract

$NaGd(MO_4)_2$:R (M = W, Mo, R = Eu^{3+}, Sm^{3+}, Bi^{3+}) phosphors were synthesized by solid-state reaction. The structure and photoluminescence properties of the samples were characterized using X-ray powder diffraction and fluorescence spectrophotometry. The $^5D_0 \rightarrow {}^7F_2$ transition of Eu^{3+}, which led to a red emission of the phosphors, was dominantly observed in the photoluminescence spectra. The doped Bi^{3+} and Sm^{3+} efficiently sensitized the emission of Eu^{3+} and effectively extended and strengthened the absorption of near-UV light with wavelengths ranging from 395 to 405 nm. In addition, energy transfers from Bi^{3+} to Eu^{3+} and from Sm^{3+} to Eu^{3+} occurred. The chromaticity coordinates of the obtained phosphors were close to the standard values of the National Television Standard Committee ($x=0.670$, $y=0.330$). The results suggest that $NaGd(WO_4)_{2-y}(MoO_4)_y$:$Eu^{3+}$, Sm^{3+}, Bi^{3+} is an efficient red-emitting phosphor for light-emitting diode applications.

Keywords: Luminescence; Phosphor; Solid-state reaction

1. Introduction

White light-emitting diode (LED) is a promising light source due to its many advantages, including low power consumption, low voltage, long service life, high reliability, environmental friendliness, and high energy efficiency. Nowadays, use of near-UV LED chips to excite trichromatic phosphors based on red, green, and blue phosphors is an acceptable solution because of their better chromogenic performance and low cost [1–3]. However, red-emitting phosphors, the key phosphors that adjust chromogenic performance and color temperature to obtain high-purity white light, actually hinder large-scale applications of white LED [4,5]. Therefore, new red phosphors that can be excited efficiently under the near-UV range of approximately 400 nm with intense emission and appropriate Commission Internationale de L'Eclai (CIE) chromaticity coordinates need to be identified.

Two approaches can be used to broaden the absorption of phosphors for near-UV LED at approximately 400 nm [6]: The first approach involves co-doping Sm^{3+} and Eu^{3+} ions in the phosphor, because Sm^{3+}/Eu^{3+} ions present strong absorption at approximately 405/395 nm and absorptions at approximately 400 nm are expected to be broadened and strengthened. The second approach, from the viewpoint of the host compound, entails that each spectroscopic line is generally expected to become narrow when rare earth ions enter the lattice sites of a pure host compound. Tungstate and molybdate adopt a scheelite structure in which sodium and rare earth ions are disordered in the same site. Mo^{6+} and W^{6+} are coordinated by four oxygen atoms in a tetrahedral site, and the rare earth/sodium site is eight coordinated, with two sets of rare oxygen distances; the similar ionic radii of tetrahedral Mo^{6+} (0.041 nm) and W^{6+} (0.042 nm) render it possible to prepare solid solutions of the type $NaGd(WO_4)_{2-x}(MoO_4)_x$ [7–9]. The intensity of the $^5D_0 \rightarrow {}^7F_2$ emission of Eu^{3+} activated at a wavelength of 396 nm has been reported to increase for $MEu(WO_4)_{2-x}(MoO_4)_x$ (M = Li, Na, K) when Mo^{6+} was introduced to replace W^{6+} [10,11].

*Corresponding author: Tel./fax: +86 771 3233718.
E-mail address: zhouliyatf@163.com (L. Zhou).

0272-8842/$36.00
http://dx.doi.org/10.1016/j.ceramint.2012.04.084

In light of the above-described approaches, this study prepared $NaGd(WO_4)_{2-x}(MoO_4)_x:Eu^{3+}$, Sm^{3+} phosphors by solid-state reaction and analyzed their luminescence. Moreover, Bi^{3+} was introduced as a co-activator to the $NaGd(WO_4)_2:Eu^{3+}$ phosphor to strengthen and broaden the absorption at approximately 400 nm [12,13].

2. Materials and methods

2.1. Synthesis

The phosphors were prepared by traditional solid-state reaction. WO_3 (A.R. grade), MoO_3 (A.R. grade), Na_2CO_3 (A.R. grade), Bi_2O_3 (A.R. grade), Sm_2O_3 (99.99%), Gd_2O_3 (99.99%), and Eu_2O_3 (99.99%) were explored as starting materials. Calculated raw materials were mixed homogeneously in an agate mortar and calcined at 900 °C for 5 h.

2.2. Characterization

The structures were identified by X-ray powder diffraction (XRD; $CuK_\alpha = 1.5406$ Å; Rigaku/Dmax 2500, Rigaku Corporation, Japan). Excitation and emission spectra were recorded using a Hitachi F-2500 fluorescence spectrophotometer with a Xe lamp as the excitation source. All measurements were carried out at room temperature.

3. Results and discussion

3.1. XRD characterization

The crystal structure of the double tungstate and molybdate compound $AB(MO_4)_2$ (A = Li^+, Na^+, K^+, Rb^+, Cs^+; B = trivalent rare earth ions) is similar to that of $CaMoO_4$, with the $[MO_4^{2-}]$ oxyanion complex as the principal constitutive element. The central M metal ion is coordinated by four O^{2-} ions in tetrahedral symmetry ($I4_1/a$) [8]. The XRD patterns of $NaGd_{0.95}(WO_4)_2:Eu^{3+}_{0.05}$ and $NaGd_{0.95}(MoO_4)_2:Eu^{3+}_{0.05}$ calcined at 900 °C are shown in Fig. 1. The figure also shows that all diffraction peaks matched the standard data of JCPDS 25-0829 [$NaGd(WO_4)_2$] well. The XRD patterns of $NaGd_{0.95}(MoO_4)_2:Eu^{3+}_{0.05}$ demonstrated that the phosphor is of single phase and consistent with JCPDS 25-0828 [$Na_{0.5}Gd_{0.5}MoO_4$] when the sample was calcined at 900 °C and that the doped Eu ion has little influence on the host structure. Due to their different valence states and differences in ion sizes between Eu^{3+} (0.107 nm) and Na^+ (0.118 nm), Eu^{3+} was expected to occupy the Gd^{3+} (0.105 nm) site in these phosphors.

3.2. Photoluminescent properties of $NaGd_{1-x}WO_4:Eu^{3+}_x$

Fig. 2 shows the excitation and emission spectra of the $NaGd_{0.50}(WO_4)_2:Eu^{3+}_{0.50}$ phosphor. Specifically, it illustrates that the excitation spectrum has two wide bands centered at 272 and 395 nm when emission was monitored at 616 nm. The band at approximately 272 nm is attributed to the

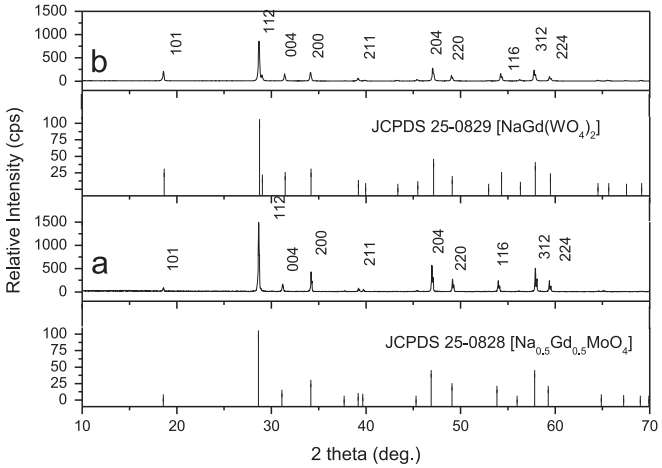

Fig. 1. XRD patterns of $NaGd_{0.95}(WO_4)_2:Eu^{3+}_{0.05}$ and $NaGd_{0.95}(MoO_4)_2:Eu^{3+}_{0.05}$.

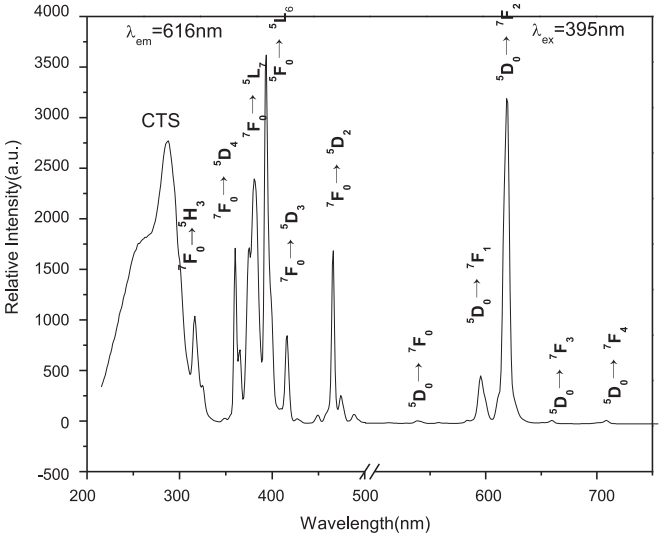

Fig. 2. Excitation ($\lambda_{em}=616$ nm; left) and emission ($\lambda_{ex}=395$ nm; right) spectra of $NaGd_{0.50}(WO_4)_2:Eu^{3+}_{0.50}$.

charge transfer (CT) state of the O–W and O–Eu^{3+} interactions [14]. The band at approximately 395 nm is ascribed to the intraconfigurational 4f–4f transitions of Eu^{3+} in the tungstate, and the strongest peak was at 395 nm ($^7F_0 \rightarrow {}^5L_6$), indicating that $NaGd_{0.50}(WO_4)_2:Eu^{3+}_{0.50}$ can be excited by InGaN chips efficiently. Under excitation at 395 nm of UV light, the emission spectrum is described by the $^5D_0$ level to ^7F_J ($J=0$, 1, 2, 3, 4) line emissions of the Eu^{3+} ions. The magnetic dipole-allowed $^5D_0 \rightarrow {}^7F_1$ transition at 593 nm was observed when the Eu^{3+} ion occupied the site with center of symmetry. The emission line at 616 nm corresponded to the electric dipole-forbidden $^5D_0 \rightarrow {}^7F_2$ transition of the Eu^{3+} ion, and this transition was observed when the Eu^{3+} ion was located in an asymmetrical cation environment [15]. As shown in Fig. 2, the luminescence intensity of the $^5D_0 \rightarrow {}^7F_2$ transition was much stronger than that of the $^5D_0 \rightarrow {}^7F_1$ transition, suggesting that the Eu^{3+} ion occupied the site without center of symmetry.

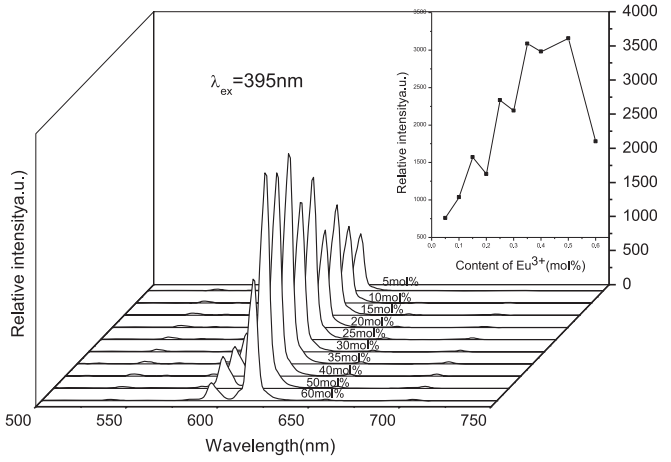

Fig. 3. Emission (λ_{ex}=395 nm) spectra of $NaGd_{1-x}(WO_4)_2:Eu^{3+}_x$ phosphors. The inset shows the effects of the Eu^{3+}-doped concentrations on the phosphors.

The effects of the Eu^{3+}-doped concentrations in the $NaGd_{1-x}(WO_4)_2:Eu^{3+}_x$ (x=0.05, 0.10, 0.15, 0.20, 0.25, 0.30, 0.35, 0.40, 0.50, 0.60) phosphors on the relative photoluminescent (PL) intensity are shown in Fig. 3. All emission spectra except for relative intensity exhibited a similar shape. The optimal doping concentration had to be confirmed to obtain the maximum luminescent intensity. Due to their different structures in various host materials, the optimal doping concentrations for the Eu ions differed. Fig. 3 (inset) shows the dependence of the integrated emission intensity on the doping concentration of Eu^{3+}. It illustrates that the emission intensity first increased with an increase in the doping concentration, reached its maximum when x=0.50, and then decreased. This quenching process is often attributable to the fact that the energy of electron in an excited state will be transmitted to the quenching center more easily when the concentration of Eu^{3+} has reached a certain value [16–20]. The chromaticity coordinates of the phosphor $NaGd_{0.50}(WO_4)_2:Eu^{3+}_{0.50}$ (λ_{ex}=395 nm) were calculated to be x=0.663, y=0.337, which are close to the standard values of the National Television Standard Committee (NTSC) (x=0.670, y=0.330).

3.3. Photoluminescent properties of $NaGd_{0.50}(WO_4)_{2-y}(MoO_4)_y:Eu^{3+}_{0.50}$ phosphors

Fig. 4 shows the emission spectra of $NaGd_{0.50}(WO_4)_{2-y}(MoO_4)_y:Eu^{3+}_{0.50}$ (y=0, 0.40, 0.80, 1.20, 1.60, 2.00) phosphors. Compared with the emission spectrum of $NaGd_{0.50}(WO_4)_2:Eu^{3+}_{0.50}$, the relative intensity of the $^5D_0 \rightarrow {}^7F_2$ emission of Eu^{3+} at 616 nm increased with increasing Mo^{6+} concentration and reached its maximum when y=0.80. The luminescence intensity decreased at Mo^{6+} concentrations higher than 0.80, indicating that an opportune amount of MoO_4^{2-} can enhance the emission intensity in $NaGd_{0.50}(WO_4)_2:Eu^{3+}_{0.50}$. The fact that non-radiative relaxation between neighboring Eu^{3+} ions is much stronger

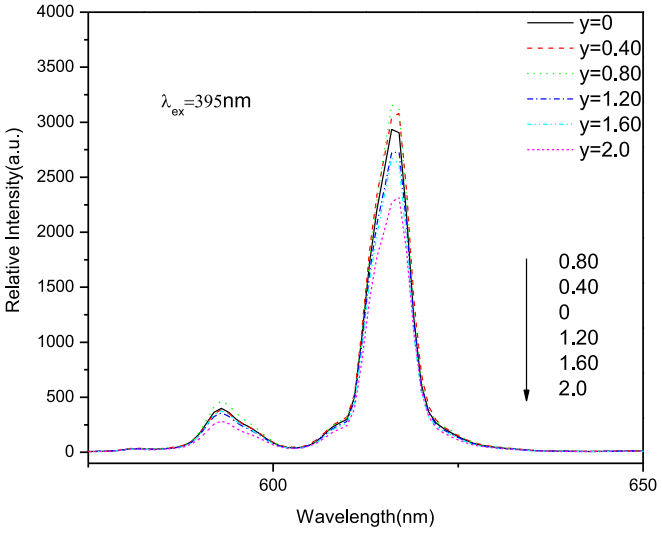

Fig. 4. Emission (λ_{ex}=395 nm) spectra of $NaGd_{0.50}(WO_4)_{2-y}(MoO_4)_y:Eu^{3+}_{0.50}$ phosphors.

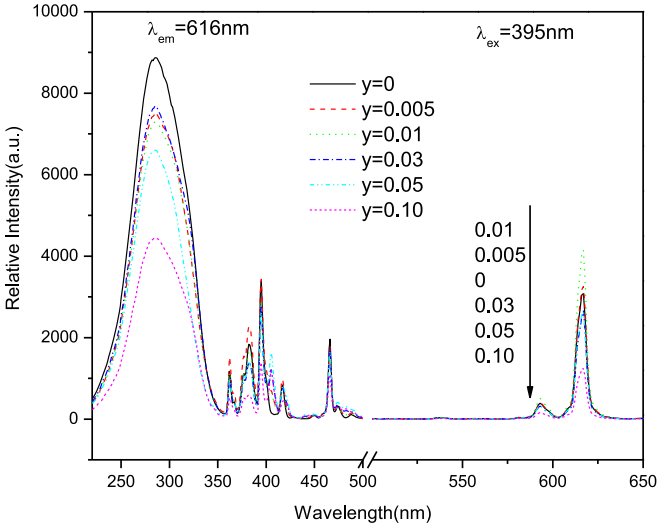

Fig. 5. Excitation (λ_{em}=616 nm) and emission (λ_{ex}=395 nm) spectra of $NaGd_{0.50-y}(WO_4)_{0.40}(MoO_4)_{1.60}:Eu^{3+}_{0.50}$, Sm^{3+}_y phosphors.

in molybdate than in tungstate can account for these results [21–23]. The chromaticity coordinates of $NaGd_{0.50}(WO_4)_{1.20}(MoO_4)_{0.80}:Eu^{3+}_{0.50}$ (λ_{ex}=395 nm) were calculated to be x=0.664, y=0.336, which are close to the standard values of the NTSC (x=0.670, y=0.330).

3.4. Photoluminescent properties of $NaGd_{0.50-y}(WO_4)_{1.20}(MoO_4)_{0.80}:Eu^{3+}_{0.50}$, Sm^{3+}_y

Fig. 5 shows the excitation and emission spectra of Sm^{3+} co-doped in $NaGd_{0.50-y}(WO_4)_{1.20}(MoO_4)_{0.80}:Eu^{3+}_{0.50}$, Sm^{3+}_y (y=0, 0.005, 0.01, 0.03, 0.05, 0.10) phosphors. At 616 nm of emission, the broad band in the range of 250–350 nm was assignable to the O→W or O→Mo CT transition, whereas the lines in the range of 360–550 nm

belonged to f–f transitions of Eu^{3+} and Sm^{3+} ions in the host lattices. The $^7F_0 \rightarrow {}^5L_6$ and $^7F_0 \rightarrow {}^5D_2$ transitions of Eu^{3+} at 395 and 466 nm were two of the strongest absorptions. The line at 405 nm was caused by the $^6H_{5/2} \rightarrow {}^4K_{11/2}$ transition of Sm^{3+} [24]. The emission intensity clearly increased with increasing Sm^{3+} concentration and reached its maximum when $y=0.01$, and the emission intensity of $NaGd_{0.49}(WO_4)_{1.20}(MoO_4)_{0.80}:Eu^{3+}_{0.50}$, $Sm^{3+}_{0.01}$ under 395 nm of excitation was 1.32 times stronger than that of $NaGd_{0.50}(WO_4)_{1.20}(MoO_4)_{0.80}:Eu^{3+}_{0.50}$. In the Eu^{3+}–Sm^{3+} co-doped system, the characteristic emissions of Eu^{3+} under 395 nm of excitation could be dominantly observed; in contrast, the $^4G_{5/2} \rightarrow {}^6H_J$, ($J=5/2$, 7/2, 9/2) intra-4 f transitions of Sm^{3+} ion at approximately 570, 610, and 650 nm were not observable. These findings demonstrate that the Sm^{3+} ions can absorb energy and efficiently transfer it to the Eu^{3+} ions [25–28].

3.5. Photoluminescent properties of $NaGd_{0.49-y}(WO_4)_{1.20}(MoO_4)_{0.80}:Eu^{3+}_{0.50}$, $Sm^{3+}_{0.01}$, Bi^{3+}_y phosphors

The excitation and emission spectra of $NaGd_{0.49-y}(WO_4)_{1.20}(MoO_4)_{0.80}:Eu^{3+}_{0.50}$, $Sm^{3+}_{0.01}$, Bi^{3+}_y ($y=0$, 0.05, 0.10, 0.15, 0.20) phosphors are shown in Fig. 6. The figure illustrates that the width of the peak at the CT bands of $Mo \rightarrow O^{2-}$ and $W \rightarrow O^{2-}$ centered at ~288 nm widened from 350–370 nm, which could be assigned to the $Bi^{3+} \rightarrow O^{2-}$ CT band and the self-absorption of Bi^{3+} from ground state $^1S_0$ to the excited state $^3P_1$ [29–31]. Compared with the emission spectrum of $NaGd_{0.49}(WO_4)_{1.20}(MoO_4)_{0.80}:Eu^{3+}_{0.50}$, $Sm^{3+}_{0.01}$, the shape and location at 593 and 616 nm remained unchanged with the introduction of Bi^{3+}, except for emission intensity. The emission intensity of $NaGd_{0.49-y}(WO_4)_{1.20}(MoO_4)_{0.80}:Eu^{3+}_{0.50}$, $Sm^{3+}_{0.01}$, Bi^{3+}_y phosphors gradually increased with increasing doped Bi^{3+} content but subsequently decreased, with the value reaching the maximum when $y=0.05$. The luminescence intensity decreased when the Bi^{3+} doping ratio exceeded 5 mol%. At very low content, the sensitization from Bi^{3+} to Eu^{3+} increased with increased Bi^{3+} content. After reaching the maximum, the energy transfer between Bi^{3+} ions became less efficient; therefore, higher Bi^{3+} doping concentrations dissipated the absorbed energy non-radiatively instead of transferring the absorbed energy from Bi^{3+} to Eu^{3+}, resulting in less energy transfer from Bi^{3+} to Eu^{3+} [32–34].

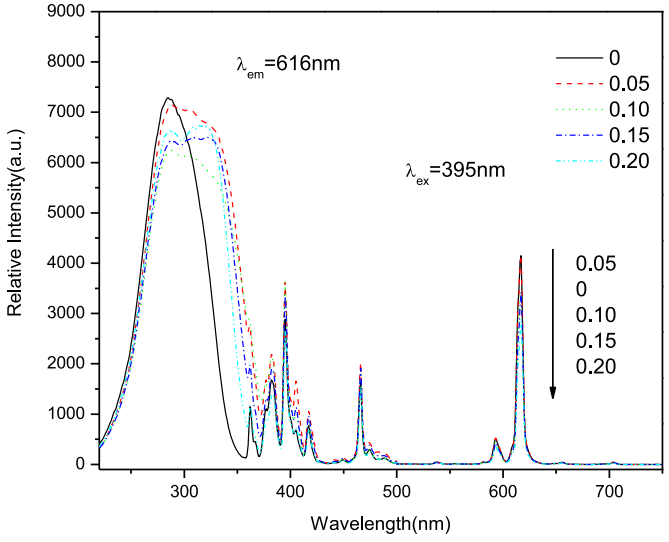

Fig. 6. Excitation ($\lambda_{em}=616$ nm; left) and emission ($\lambda_{ex}=395$ nm; right) spectra of $NaGd_{0.49-y}(WO_4)_{1.20}(MoO_4)_{0.80}:Eu^{3+}_{0.50}$, $Sm^{3+}_{0.01}$, Bi^{3+}_y phosphors.

The CIE chromaticity coordinates of $NaGd(MO_4)_2$:R (M = W, Mo, R = Eu^{3+}, Sm^{3+}, Bi^{3+}) phosphors are listed in Table 1. The chromaticity coordinates of $NaGd_{0.50}(WO_4)_2:Eu^{3+}_{0.50}$, $NaGd_{0.50}(WO_4)_{1.20}(MoO_4)_{0.80}:Eu^{3+}_{0.50}$, $NaGd_{0.49}(WO_4)_{1.20}(MoO_4)_{0.80}:Eu^{3+}_{0.50}$, $Sm^{3+}_{0.01}$, and $NaGd_{0.44}(WO_4)_{1.20}(MoO_4)_{0.80}:Eu^{3+}_{0.50}$, $Sm^{3+}_{0.01}$, $Bi^{3+}_{0.05}$ approximated NTSC standard values. The $NaGd_{0.49-y}(WO_4)_{1.20}(MoO_4)_{0.80}:Eu^{3+}_{0.50}$, $Sm^{3+}_{0.01}$, Bi^{3+}_y phosphors broadened the absorption band at approximately 400 nm and strengthened emission with good CIE chromaticity coordinates.

3.6. Fabrication of LED with the phosphors

The emission spectra of the original 395 nm-emitting InGaN chip and the red-emitting LED with $NaGd_{0.50}(WO_4)_2:Eu^{3+}_{0.50}$, $NaGd_{0.50}(WO_4)_{1.20}(MoO_4)_{0.80}:Eu^{3+}_{0.50}$, $NaGd_{0.49}(WO_4)_{1.20}(MoO_4)_{0.80}:Eu^{3+}_{0.50}$, $Sm^{3+}_{0.01}$, and $NaGd_{0.44}(WO_4)_{1.20}(MoO_4)_{0.80}:Eu^{3+}_{0.50}$, $Sm^{3+}_{0.01}$, $Bi^{3+}_{0.05}$ under 20 mA of forward bias are shown in Fig. 7. The band at approximately 395 nm resulted from the emission of the InGaN chip, and the shoulder peak located at approximately 390 nm was caused by the absorption of the red phosphor. The sharp peaks at 593, 616, 655, and 703 nm originated from the emission of the coated phosphors $NaGd_{0.50}(WO_4)_2:Eu^{3+}_{0.50}$, $NaGd_{0.50}(WO_4)_{1.20}(MoO_4)_{0.80}:Eu^{3+}_{0.50}$, $NaGd_{0.49}(WO_4)_{1.20}(MoO_4)_{0.80}:Eu^{3+}_{0.50}$, $Sm^{3+}_{0.01}$, and $NaGd_{0.44}(WO_4)_{1.20}(MoO_4)_{0.80}:Eu^{3+}_{0.50}$, $Sm^{3+}_{0.01}$, $Bi^{3+}_{0.05}$, respectively. The results demonstrated that the $NaGd_{0.44}(WO_4)_{1.20}(MoO_4)_{0.80}:Eu^{3+}_{0.50}$, $Sm^{3+}_{0.01}$, $Bi^{3+}_{0.05}$ phosphor could efficiently absorb the ~400 nm excitation energy that the InGaN chip emitted, thereby making it a good candidate for the red component of trichromatic white LED applications.

4. Conclusions

The red phosphors $NaGd(WO_4)_2:Eu^{3+}$, $NaGd(WO_4)_{2-y}(MoO_4)_y:Eu^{3+}$, $NaGd(WO_4)_{2-y}(MoO_4)_y:Eu^{3+}$, Sm^{3+}, and $NaGd(WO_4)_{2-y}(MoO_4)_y:Eu^{3+}$, Sm^{3+}, Bi^{3+} were synthesized by solid-state reaction. The doped Sm^{3+} and Bi^{3+} proved efficient in sensitizing the emission of Eu^{3+} and extending the absorption of near-UV light with wavelengths at approximately 400 nm. As the non-radiative relaxation between the neighboring Eu^{3+} ions was much stronger in molybdate than in tungstate, the optimum Mo^{6+} concentration was 0.80. Only the characteristic transition emissions of Eu^{3+} were detected, indicating that the co-doped Bi^{3+} and Sm^{3+} ions absorbed and transferred energy to Eu^{3+} ions efficiently. In addition,

Table 1
CIE chromaticity coordinates of $NaGd(MO_4)_2$:R (M=W, Mo, R=Eu^{3+}, Sm^{3+}, Bi^{3+}) phosphors.

Sample	Excitation (nm)	CIE chromaticity coordinates	
		x	*y*
$NaGd_{0.95}(WO_4)_2:Eu^{3+}_{0.05}$	395	0.660	0.340
$NaGd_{0.90}(WO_4)_2:Eu^{3+}_{0.10}$	395	0.661	0.339
$NaGd_{0.85}(WO_4)_2:Eu^{3+}_{0.15}$	395	0.661	0.338
$NaGd_{0.80}(WO_4)_2:Eu^{3+}_{0.20}$	395	0.661	0.339
$NaGd_{0.75}(WO_4)_2:Eu^{3+}_{0.25}$	395	0.662	0.338
$NaGd_{0.70}(WO_4)_2:Eu^{3+}_{0.30}$	395	0.662	0.338
$NaGd_{0.65}(WO_4)_2:Eu^{3+}_{0.35}$	395	0.662	0.338
$NaGd_{0.60}(WO_4)_2:Eu^{3+}_{0.40}$	395	0.662	0.337
$NaGd_{0.50}(WO_4)_2:Eu^{3+}_{0.50}$	395	0.663	0.337
$NaGd_{0.40}(WO_4)_2:Eu^{3+}_{0.60}$	395	0.663	0.337
$NaGd_{0.50}(WO_4)_{1.60}(MoO_4)_{0.40}:Eu^{3+}_{0.50}$	395	0.663	0.337
$NaGd_{0.50}(WO_4)_{1.20}(MoO_4)_{0.80}:Eu^{3+}_{0.50}$	395	0.664	0.336
$NaGd_{0.50}(WO_4)_{0.80}(MoO_4)_{0.1.20}:Eu^{3+}_{0.50}$	395	0.664	0.336
$NaGd_{0.50}(WO_4)_{0.40}(MoO_4)_{1.60}:Eu^{3+}_{0.50}$	395	0.664	0.335
$NaGd_{0.50}$ $(MoO_4)_2:Eu^{3+}_{0.50}$	395	0.664	0.335
$NaGd_{0.495}(WO_4)_{0.40}(MoO_4)_{1.60}:Eu^{3+}_{0.50}$, $Sm^{3+}_{0.005}$	395	0.665	0.335
$NaGd_{0.49}(WO_4)_{0.40}(MoO_4)_{1.60}:Eu^{3+}_{0.50}$, $Sm^{3+}_{0.01}$	395	0.665	0.335
$NaGd_{0.47}(WO_4)_{0.40}(MoO_4)_{1.60}:Eu^{3+}_{0.50}$, $Sm^{3+}_{0.03}$	395	0.657	0.341
$NaGd_{0.45}(WO_4)_{0.40}(MoO_4)_{1.60}:Eu^{3+}_{0.50}$, $Sm^{3+}_{0.05}$	395	0.664	0.336
$NaGd_{0.40}(WO_4)_{0.40}(MoO_4)_{1.60}:Eu^{3+}_{0.50}$, $Sm^{3+}_{0.10}$	395	0.663	0.337
$NaGd_{0.44}(WO_4)_{0.40}(MoO_4)_{1.60}:Eu^{3+}_{0.50}$, $Sm^{3+}_{0.01}$,$Bi^{3+}_{0.05}$	395	0.665	0.335
$NaGd_{0.39}(WO_4)_{0.40}(MoO_4)_{1.60}:Eu^{3+}_{0.50}$, $Sm^{3+}_{0.01}$,$Bi^{3+}_{0.10}$	395	0.665	0.335
$NaGd_{0.34}(WO_4)_{0.40}(MoO_4)_{1.60}:Eu^{3+}_{0.50}$, $Sm^{3+}_{0.01}$,$Bi^{3+}_{0.15}$	395	0.664	0.335
$NaGd_{0.29}(WO_4)_{0.40}(MoO_4)_{1.60}:Eu^{3+}_{0.50}$, $Sm^{3+}_{0.01}$,$Bi^{3+}_{0.20}$	395	0.664	0.336

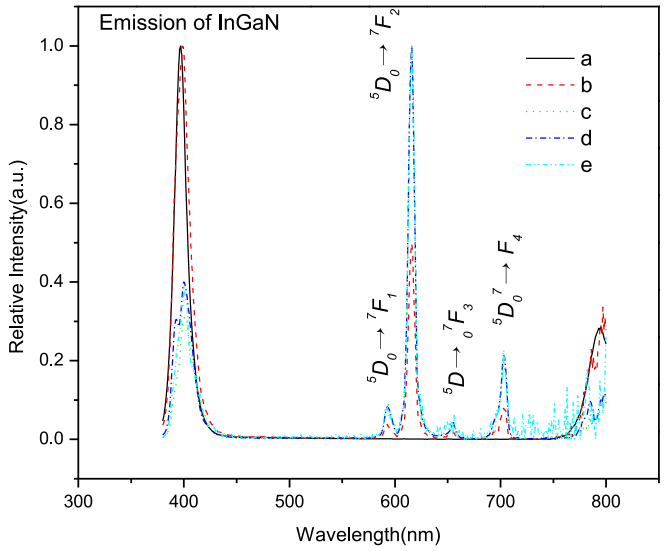

Fig. 7. Emission spectra of (a) the original 395 nm-emitting InGaN chip and (b–e) the red-emitting LED with (b) $NaGd_{0.50}(WO_4)_2:Eu^{3+}_{0.50}$, (c) $NaGd_{0.50}(WO_4)_{1.20}(MoO_4)_{0.80}:Eu^{3+}_{0.50}$, (d) $NaGd_{0.49}(WO_4)_{1.20}(MoO_4)_{0.80}$:$Eu^{3+}_{0.50}$, $Sm^{3+}_{0.01}$, and (e) $NaGd_{0.44}(WO_4)_{1.20}(MoO_4)_{0.80}:Eu^{3+}_{0.50}$, $Sm^{3+}_{0.01}$, $Bi^{3+}_{0.05}$. (For interpretation of the references to color in this figure legend, the reader is referred to the web version of this article.)

the chromaticity coordinates of $NaGd_{0.50}(WO_4)_2:Eu^{3+}_{0.50}$, $NaGd_{0.50}(WO_4)_{1.20}(MoO_4)_{0.80}:Eu^{3+}_{0.50}$, $NaGd_{0.49}(WO_4)_{1.20}(MoO_4)_{0.80}:Eu^{3+}_{0.50}$, $Sm^{3+}_{0.01}$, and $NaGd_{0.44}(WO_4)_{1.20}(MoO_4)_{0.80}$:$Eu^{3+}_{0.50}$, $Sm^{3+}_{0.01}$, $Bi^{3+}_{0.05}$ were (x=0.663, y=0.337), (x=0.664, y=0.336), (x=0.665, y=0.335), and (x=0.665, y=0.335), respectively, which approximated the red color standard values mandated by the NTSC. This study has demonstrated that the above-described phosphors hold considerable potential in white LED applications.

Acknowledgments

This work was financially supported by grants from the National Natural Science Foundation of China (no. 61066006), Science Foundation of Guangxi Province (no. 2011GXNSFA018054).

References

[1] M. Mikami, N. Kijima, B. Bertrand, M. Stankovski, X. Gonze, Theoretical approach for white-LED phosphors: from crystal structures to optical properties, Materials Science and Engineering 18 (2011) 1–6.
[2] S. Nishiura, S. Tunabe, K. Fujioka, Y. Fujimoto, Properties of transparent Ce:YAG ceramic phosphors for white LED, Optical Materials 33 (2011) 688–691.
[3] Q.L. Dai, M.E. Foley, C.J. Breshike, A. Lita, G.F. Strouse, Ligand-passivated Eu:Y_2O_3 nanocrystals as a phosphor for white light emitting diodes, Journal of the American Chemical Society 133 (2011) 15475–15486.
[4] C.C. Lin, R.S. Liu, Advances in phosphors for light-emitting diodes, The Journal of Physical Chemistry Letters 2 (2011) 1268–1277.
[5] Y. Yan, F.B. Cao, Y.W. Tian, L.S. Li, Improved luminescent properties of red-emitting $Ca_{0.54}Sr_{0.16}Gd_{0.12}(MoO_4)_{0.2}(WO_4)_{0.80}$ phosphor for LED application by charge compensation, Journal of Luminescence 131 (2011) 1140–1143.

[6] Z.L. Wang, H.B. Liang, L.Y. Zhou, H. Wu, M.L. Gong, Q. Su, Luminescence of near UV InGaN-based light-emitting diode, Chemical Physics Letters 412 (2005) 313–316.
[7] A. Kumar, J. Kumar, Perspective on europium activated fine-grained metal molybdate phosphors for solid state illumination, Journal of Materials Chemistry 21 (2011) 3788–3795.
[8] F.B. Cao, L.S. Li, T.W. Tian, Z.F. Gao, Y.J. Chen, L.J. Xiao, X.R. Wu, Sol–gel synthesis of red-phosphors [$NaxG_{1-x/3-z}Eu_z$]$Mo_yW_{1-y}O_4$ power and luminescence properties, Optical Materials 33 (2011) 751–754.
[9] H. Lin, Y. Zhang, C. Li, F.M. Zeng, X.J. Zhang, M. Tonelli, J.H. Liu, Study of $NaM(WO_4)_2$ crystal growth and property(M: Gd^{3+}, Bi^{3+}), Sciene of Advanced Materials 2 (2010) 489–492.
[10] B. Yan, L.X. Lin, J.H. Wu, F. Lei, Photoluminescence of rare earth phosphors $Na_{0.5}Gd_{0.5}WO_4$: RE^{3+} and $NaGd_{0.5}(Mo_{0.75}W_{0.25})O_4$: RE^{3+}(RE=Eu, Sm, Dy), Journal of Fluorescence 21 (2011) 203–211.
[11] F.B. Cao, L.S. Li, Y.W. Tian, Y.J. Chen, X.R. Wu, Investigation of red-emission phosphors (Ca,Sr)(Mo,W)O:Eu^{3+} crystal structure, luminous characteristics and calculation of $Eu^{3+5}D_0$ quantum efficiency, Thin Solid Films 519 (2011) 7971–7976.
[12] A. Xie, X.M. Yuan, Y. Shi, F.X. Wang, J.J. Wang, Photoluminescence characteristics of energy transfer between Eu^{3+} and Bi^{3+} in $LiEu_{1-x}Bi_x(WO_4)_{0.5}(MoO_4)_{1.5}$, Journal of the American Ceramic Society 92 (2009) 2254–2258.
[13] S. Neeraj, N. Kijima, A.K. Cheetham, Novel red phosphors for solid-state lighting: the system $NaM(WO_4)_{2-x}(MoO_4)_x$:Eu^{3+}(M=Gd, Y, Bi), Chemical Physics Letters 387 (2004) 2–6.
[14] L.X. Yu, H. Liu, The progress of photoluminescent properties of rare-earth-ions-doped phosphate one-dimensional nanocrystals, Journal of Nanomaterials 2 (2010) 1–6.
[15] J.B. Gruber, U.V. Valieve, G.W. Burdick, S.A. Rakhimov, M. Pokhrel, D.K. Sardar, Spectra energy levels, and symmetry assignments for stark components of $Eu^{3+}(4f^6)$ in gadolinium gauium garnet($Gd_3Ga_5O_{12}$), Journal of Luminescence 131 (2011) 1945–1952.
[16] Y. Tian, B.J. Chen, R.N. Hua, J.S. Sun, L.H. Cheng, Optical transition electron–phonon coupling and fluorescent quenching of $La_2(MoO_4)_3$:Eu^{3+} phosphors, Journal of Applied Physics 109 (2011) 053511-1–053511-6.
[17] Z.H. Ju, R.P. Wei, X.P. Gao, W.S. Liu, C.R. Pang, Red phosphor $SrWO_4$:Eu^{3+} for potential application in white LED, Optical Materials 33 (2011) 909–913.
[18] Y.R. Do, Y.D. Huh, Optical properties of potassium europium tungstate phosphors, Journal of the Electrochemical Society 147 (2000) 4385–4388.
[19] C.A. Kodaira, H.F. Brito, M.C.F.C. Felinto, Luminescence investigation of Eu^{3+} ion in the $RE_2(WO_4)_3$ matrix (RE=La and Gd) produced using the Pechini method, Journal of Solid State Chemistry 171 (2003) 401–407.
[20] H.Y. Jiao, Y.H. Wang, Intense red phosphors for near-ultraviolet light-emitting diodes, Applied Physics B: Lasers and Optics 98 (2010) 423–427.
[21] X.X. Wang, Y.L. Xian, J.X. Shi, Q. Su, M.L. Gong, The potential red emitting $Gd_{2-y}Eu_y(WO_4)_{3-x}(MoO_4)_x$ phosphors for UV InGaN-base light-emitting diode materials, Materials Science and Engineering B 144 (2007) 69–72.
[22] C.H. Chiu, M.F. Wang, C.S. Lee, T.M. Chen, Structure, spectroscopic and photoluminescence studies of $LiEu(WO_4)_{2-x}(MoO_4)_x$ as a near-UV convertible phosphor, Journal of Solid State Chemistry 180 (2007) 619–627.
[23] X.L. Gao, Y.H. Wang, D. Wang, B.T. Liu, Luminescent properties of $KGd_{1-x}(WO_4)_2$:Eu_x^{3+} and $KGd_{1-x}(WO4)_{2-y}(MoO_4)_y$:$Eu_x^{3+}$ phosphors in UV–VUV regions, Journal of Luminescence 129 (2009) 840–843.
[24] Y.H. Zhou, J. Lin, S.B. Wang, Energy transfer and upconversion luminescence properties of Y_2O_3:Sm and Gd_2O_3:Sm phosphors, Journal of Solid-State Chemistry 171 (2003) 391–395.
[25] A. Nag, T.R.N. Kutty, Photoluminescence of $Sr_{2-x}Ln_xCeO_{4+x/2}$ (Ln∼Eu, Sm or Yb) prepared by a wet chemical method, Journal of Materials Chemistry 13 (2003) 370–376.
[26] Z.L. Wang, H.B. Liang, M.L. Gong, Q. Su, Novel red phosphor of Bi^{3+}, Sm^{3+} co-acivated $NaEu(MoO_4)_2$, Optical Materials 29 (2007) 896–900.
[27] X.S. Yan, W.W. Li, K. Sun, A novel emitting phosphor $CaInO_4$:Eu^{3+}, Sm^{3+} with a broadened near-ultraviolet absorption band for solid-state lighting, Materials Research Bulletin 46 (2011) 87–91.
[28] Z.L. Wang, H.B. Liang, L.Y. Zhou, J. Wang, M.L. Gong, Q. Su, $NaEu_{0.96}Sm_{0.04}(MoO_4)_2$ as a promising red-emitting phosphor for LED solid-state lighting prepared by the Pechini process, Journal of Luminescence 128 (2008) 147–154.
[29] B. Yan, J.H. Wu, $NaY(MoO_4)_2$:Eu^{3+} and $NaY_{0.90}Bi_{0.10}(MoO_4)_2$:$Eu^{3+}$ submicrometer phosphors: hydrothermal synthesis assisted by room tempreature-solid state reaction, microstructure and photoluminescence, Materials Chemistry and Physics 116 (2009) 67–71.
[30] X.T. Chen, Y.H. Chen, X.R. Cheng, M. Yin, W. Xu, Photoluminescence characterristics and energy transfer bettween Bi^{3+} and Eu^{3+} in Gd_2O_3:Eu^{3+}, Bi^{3+} nanophosphors, Applied Physics B: Lasers and Optics 99 (2010) 763–768.
[31] R.B. Pode, S.J. Dhoble, Photoluminescence in CaWO4:Bi^{3+}, Eu^{3+} material, Physica Status Solidi (b) 203 (1997) 571–577.
[32] J.H. Hong, Z.G. Zhang, C.J. Cong, K.L. Zhang, Energy transfer from Bi^{3+} sensitizing and luminescence of Eu^{3+} in clusters embeded into sol–gel silica glasses, Journal of Non-Crystalline Solids 353 (2007) 2431–2435.
[33] S.X. Yan, J.H. Zhang, X. Zhang, S.Z. Lu, X.G. Ren, Z.G. Nie, X.J. Wang, Enhance red emission in $CaMoO_4$:Bi^{3+}, Eu^3, Journal of Physical Chemistry C 111 (2007) 13256–13260.
[34] W.D. Fragoso, C.D.M. Doneg, R.L. Longo, Luminescence and energy transfer in La_2O_3–Nb_2O_5–B_2O_3:M^{3+} (M=Bi, Eu, Dy) glasses, Journal of Luminescence 105 (2003) 97–103.